Article Type:	Invited Methods Collection - JoVE Produced Video
Manuscript Number:	JoVE62155R1
Full Title:	4-dimensional imaging of zebrafish optic cup morphogenesis
Corresponding Author:	Kristen Kwan University of Utah Salt Lake City, UT UNITED STATES
Corresponding Author's Institution:	University of Utah
Corresponding Author E-Mail:	kmkwan@genetics.utah.edu
Order of Authors:	Sarah Lusk
	Macaulie Casey
	Kristen Kwan
Additional Information:	
Question	**Response**
Please specify the section of the submitted manuscript.	Neuroscience
Please indicate whether this article will be Standard Access or Open Access.	Open Access (US$4,200)
Please indicate the **city, state/province, and country** where this article will be **filmed**. Please do not use abbreviations.	Salt Lake City, Utah, United States
Please confirm that you have read and agree to the terms and conditions of the author license agreement that applies below:	I agree to the Author License Agreement
Please provide any comments to the journal here.	

TITLE:
4-Dimensional Imaging of Zebrafish Optic Cup Morphogenesis

AUTHORS AND AFFILIATIONS:
Sarah Lusk[1], Macaulie A. Casey[1], Kristen M. Kwan[1]

[1]Department of Human Genetics, University of Utah, Salt Lake City, UT, USA

Corresponding Author:
Kristen M. Kwan (kmkwan@genetics.utah.edu)

Email Addresses of Co-authors:
Sarah Lusk (sarah.lusk@utah.edu)
Macaulie Casey (macaulie.casey@utah.edu)
Kristen M. Kwan (kmkwan@genetics.utah.edu)

KEYWORDS:
imaging, microscopy, timelapse, morphogenesis, optic vesicle, optic cup, development, zebrafish, eye, retina

SUMMARY:
This protocol describes an approach for in toto labeling and multidimensional imaging of zebrafish early eye development. We describe labeling, embedding, and four dimensional (4D) imaging using laser scanning confocal microscopy, and considerations for optimizing acquisition of datasets for dissecting mechanisms of optic cup morphogenesis.

ABSTRACT:
Visual system function requires the establishment of precise tissue and organ structures. In the vertebrate eye, structural defects are a common cause of visual impairment, yet mechanisms of eye morphogenesis are still poorly understood. The basic organization of the embryonic eye is conserved throughout vertebrates, thus live imaging of zebrafish embryos has become a powerful approach to directly observe eye development at real time under normal and pathological conditions. Dynamic cell processes including movements, morphologies, interactions, division, and death can be visualized in the embryo. We have developed methods for uniform labeling of subcellular structures and timelapse confocal microscopy of early eye development in zebrafish. This protocol outlines the method of generating capped mRNA for injection into the 1-cell zebrafish embryo, mounting embryos at optic vesicle stage (~12 hours post fertilization, hpf), and performing multi-dimensional timelapse imaging of optic cup morphogenesis on a laser scanning confocal microscope, such that multiple datasets are acquired sequentially in the same imaging session. Such an approach yields data that can be used for a variety of purposes, including cell tracking, volume measurements, three-dimensional (3D) rendering, and visualization. Our approaches allow us to pinpoint the cellular and molecular mechanisms driving optic cup development, in both wild type and genetic mutant conditions.

44 These methods can be employed directly by other groups or adapted to visualize many additional
45 aspects of zebrafish eye development.
46
47 **INTRODUCTION:**
48 Vertebrate eye development begins with the emergence, or evagination, of the optic vesicles
49 from the prospective brain neuroepithelium. The optic vesicles then undergo a series of tissue
50 shape changes, elongating and then invaginating to generate the optic cup. In the optic cup, the
51 neural retina and retinal pigment epithelium, both derived from the neuroepithelium, enwrap
52 the nascent lens, which is derived from the surface ectoderm. The entire process requires a
53 complex series of cell and tissue movements and molecular signaling, coordinated between
54 neuroepithelium, ectoderm, and mesenchymal cell populations. These initial events establish the
55 basic structure of the eye, and later steps of eye development, including iris and cornea
56 formation, are elaborations on early organization. Disruptions to early eye development and
57 morphogenesis underlie numerous visual impairment conditions in humans, including
58 anophthalmia, microphthalmia, and coloboma. Unlocking the cellular and molecular mechanisms
59 governing optic cup morphogenesis is crucial for further understanding the visual system
60 development and the pathological conditions that result when these processes go awry.
61
62 Our understanding of vertebrate eye development and morphogenesis emerged from a
63 tremendous amount of work spanning classic histological studies to embryological and genetic
64 approaches in a variety of model organisms including mouse, chick, frog, and fish[1–5]. While this
65 body of work established molecular mechanisms that regulate early eye development,
66 historically there exists a poor understanding of the morphogenesis of the eye: the emergence
67 of its 3D structure. The bulk of these findings have come from imaging sectioned embryos at
68 discrete time points. While this is sufficient to provide a view of tissue morphology in 2
69 dimensions, morphogenesis is a dynamic, 3D process. In order to determine how the shape of
70 the tissue changes in 3 dimensions over time, how single cells behave, and how those behaviors
71 contribute to changes in 3D tissue shape, different approaches are necessary.
72
73 One solution to address this significant gap in knowledge is live imaging, which enables dynamic
74 observation of cells and tissues in real time as the organ takes shape. Unfortunately, this is not
75 readily feasible in many model organisms due to the constraints of embryonic development. For
76 example, mouse and chick embryos (developing in utero or within an eggshell) are not easily
77 accessed, and many live embryos are not optically transparent, causing significant light scatter
78 and limiting the depth to which images can be acquired. Zebrafish, with external development
79 and transparent embryos, provide a unique opportunity to carry out live imaging of eye
80 morphogenesis[6–19]. Ample transgenic and mutant lines are also available, as well as tools to
81 generate new transgenics and mutants[20–24]. Further, optic cup morphogenesis occurs rapidly in
82 zebrafish, over a 12 h timeframe (12–24 hours post fertilization, hpf), making imaging of the
83 entire process feasible.
84
85 Live imaging efforts have been accelerated by expansion and optimization of the family of
86 fluorescent proteins, which allow genetically encoded vital labeling of subcellular structures, as
87 well as improvements and innovations to microscopy methods. The protocol described here uses

88 laser scanning confocal microscopy, rather than other current approaches to imaging zebrafish
89 embryogenesis, including spinning disk confocal microscopy, selective plane illumination
90 microscopy (SPIM and its variants), and other more specialized microscopy methods. For the
91 developing zebrafish eye, we found that spinning disk confocal microscopy was not sufficient for
92 imaging deeper in the tissue. Although SPIM boasts an extremely fast imaging time and is
93 becoming more widely used, handling the large datasets for visualization and analysis remains a
94 challenge. In contrast, laser scanning confocal microscopy is easily accessible, especially for
95 individuals lacking expertise in assembling optical hardware. We hope that the wide availability
96 of laser scanning confocal microscopy will make our protocol useful for many labs.
97
98 Here, we describe our method for capturing 4D datasets of optic cup morphogenesis, using in
99 toto labeling of the embryo for membranes and chromatin, and a laser scanning confocal
100 microscope for image acquisition (schematized in **Figure 1**). The fluorescent proteins used here
101 (EGFP-CAAX and H2A.F/Z-mCherry) were chosen to provide tissue labeling with single cell
102 resolution. We use datasets generated with this protocol for a variety of image analysis and
103 visualization functions. This protocol can be easily adapted if other subcellular structures are
104 desired. Plasma membrane labeling was selected for visualization of cell shape: we use EGFP-
105 CAAX, in which the last 21 amino acids of H-ras, serving as a prenylation signal sequence, are
106 fused to the C-terminus of EGFP[13]. Other plasma membrane targeted fluorescent proteins (e.g.,
107 transmembrane fusion or myristoylated) are likely to work just as well. To mark nuclei, we
108 selected H2A.F/Z-mCherry, in which mCherry is fused to a histone protein[13]. This ensures that
109 cell division, including mitotic spindle orientation, is easily visualized.
110
111 With any live imaging approach, one must consider trade-offs between increasing imaging speed
112 while maximizing signal-to-noise ratio, axial resolution, and sample preservation. We have
113 optimized our methods to maximize image quality and number of embryos that can be imaged
114 in a single run. Often, the goal is to image optic cup morphogenesis in a homozygous mutant
115 embryo, which may be phenotypically indistinguishable from wild type at the onset of optic cup
116 morphogenesis and the offspring of a heterozygous incross (25% of the embryos are the desired
117 genotype). By optimizing, and then multiplexing image acquisition, there is an increased
118 likelihood of capturing a dataset of a homozygous mutant embryo.
119
120 Temporal resolution, or how frequently volume data (Z-stacks) are acquired, is a key aspect of
121 timelapse imaging. Depending on the purpose for such datasets, there are different requirements
122 for speed. Initially this protocol was developed for manual 4D cell tracking. Tracking of individual
123 cells within a uniformly labeled tissue requires high enough temporal resolution to provide
124 confidence that any one cell is being continuously tracked over time. We found that Z-stacks of
125 zebrafish optic cup morphogenesis must be acquired at least every 3.1 min over 12 h; here, we
126 have optimized our acquisition on a laser scanning confocal microscope such that we can acquire
127 Z-stacks of 4–5 embryos every 2.5 min.
128
129 Establishing Z-step size was a crucial step in protocol optimization: for 3D rendering and
130 visualization, isotropic data are ideal, in which the Z-step size is equal to XY pixel dimension. In
131 reality, it is extremely difficult to acquire such timelapse data with live samples, given constraints

132 with imaging time and photobleaching. Therefore, determining the adequate Z-step size is
133 important for the rendering and visualization needs of the experiment, and specifically, what
134 X:Y:Z voxel ratio is needed to maximize axial information while maintaining speed and preventing
135 photobleaching. For this protocol, the voxel ratio established was 1:1:3.5 (0.7 μm x 0.7 μm x 2.1
136 μm Z-step size using a 40x long working distance water immersion objective). When acquiring a
137 Z-depth of 130–140 μm, this yields volume data with suitable temporal resolution and little
138 photobleaching.
139
140 As discussed above, this protocol is specific for 4D imaging of zebrafish optic cup morphogenesis,
141 using embryos in toto labeled for plasma membrane and chromatin, and a laser scanning
142 confocal microscope. The protocol below can be easily adapted for a variety of experiments and
143 needs. First, with respect to subcellular structures, any structure for which a live cell marker exists
144 can be imaged. Next, although the focus here is exclusively on optic cup morphogenesis,
145 timelapse imaging can be adapted for other stages of eye development, for example,
146 neurogenesis[25–33]. For imaging later development, one may need to consider embryo
147 immobilization (as spontaneous muscle activity begins around 24 hpf), pigmentation (which
148 begins to emerge around 24 hpf), tissue size (the eye grows significantly in volume during
149 neurogenesis), and imaging speed (which should be adjusted depending on the speed of the
150 process of interest). All of these considerations can be readily managed. The protocol is quite
151 flexible; in addition to the details of the specific protocol here, there are general principles that
152 will aid those interested in live imaging other aspects of eye development.
153
154 **PROTOCOL:**
155 All methods described here using zebrafish are covered under Dr. Kristen Kwan's animal protocol,
156 "Cellular and Molecular Mechanisms of Visual System Development in Zebrafish", and approved
157 by the Institutional Animal Care and Use Committee (IACUC) of the University of Utah.
158
159 **1. Capped RNA Synthesis**
160
161 1.1. Generate the DNA template for in vitro transcription.
162
163 1.1.1. Linearize the DNA template by digesting 10 μg of DNA in 100 μL volume of the reaction
164 mixture. A typical reaction is assembled as follows: digest 10 μg DNA using 3 μL of enzyme and
165 10 μL of buffer, bring the reaction volume to 100 μL with water.
166
167 NOTE: A typical template for digest is a pCS2 vector, for example, pCS2-EGFP-CAAX or pCS2FA-
168 H2A.F/Z-mCherry for the membrane and chromatin labeling described here. In this case, the
169 plasmid DNAs are each digested using the enzyme NotI. Users should be cautious of star activity;
170 in this case, a high-fidelity enzyme is recommended and commercially available.
171
172 1.1.2. Incubate the reaction at 37 °C overnight to ensure that the DNA is digested to completion.
173
174 1.1.3. Clean up the restriction digest using a PCR purification kit following the manufacturer's
175 protocol. Elute the DNA with 30 μL ddH$_2$O. Store the linearized DNA at -20 °C and use as needed.

176

NOTE: The amount of DNA digested and the elution volume yield approximately 0.3 µg/µL; this is sufficient for ~5 rounds of in vitro transcription, each round using ~2 µg of DNA as template.

1.2. In vitro transcribe capped RNA using an in vitro transcription kit. For pCS2 templates (as described here), use an SP6 kit.

1.2.1. Assemble the in vitro transcription reaction, as follows: Digest 2 µg of DNA template or up to 6 µL with 2 µL of 10x Reaction Buffer, 10 µL of 2x Ribonucleotide Mix, and 2 µL of 10x Enzyme Mix.

1.2.2. Incubate at 37 °C for 2–4 h or longer (longer times will lead to greater yield). If desired, 1 µL of Enzyme Mix can be supplemented halfway through the incubation period.

1.2.3. Digest the DNA template by adding 1 µL of RNase-free DNase and incubating for 15 min at 37 °C.

1.3. Purify the capped RNA using an RNA purification kit following manufacturer's protocol (see **Table of Materials**). Elute with 100 µL of RNase-free H_2O.

NOTE: The addition of β-mercaptoethanol is not necessary for this application. While the method described in this protocol is straightforward, alternative reagents can also be used to purify RNA.

1.4. Precipitate the RNA.

1.4.1. Add 10 µL of 3 M RNase-free NaOAc and 2.5 volumes (~275 µL) of ice-cold RNase-free 100% EtOH to the eluted RNA.

1.4.2. Incubate the reaction at -20 °C for 15–30 min. Spin for 15 min at high speed at 4 °C to pellet the RNA.

NOTE: The pellet should be visible against the wall of the tube. It is helpful to note how the tube is aligned in the centrifuge at this step, in order to predict where the pellet should be at the end of the spin.

1.4.3. Remove EtOH carefully with a syringe, being careful to avoid heating, over-drying, or dislodging the pellet. Resuspend the pellet in 20 µL of RNase-free H_2O.

1.4.4. Check the RNA to ensure that the synthesis is successful. Use 1 µL to assay concentration on a spectrophotometer and run 0.5 µL on a 1% agarose gel to check for one or two discrete bands, rather than a low molecular weight smear. The yield of the in vitro transcription reaction should be ~1 µg/µL.

219 1.4.5. Aliquot and store RNA at -20 °C or -80 °C. The RNA is not diluted until immediately prior to
220 injections.
221
222 <mark>**2. Microinjection of 1-cell zebrafish embryos**</mark>
223
224 NOTE: Inject 200–300 pg per RNA to obtain ubiquitous expression of chromatin and cell
225 membranes throughout optic cup morphogenesis. Prepare 5–10 µL of the RNA dilution, and load
226 2.5–5 µL/needle; plan for extra in the event the needle breaks.
227
228 2.1. Advance preparations for injections.
229
230 2.1.1. Prepare an injection mold dish to facilitate alignment and orientation of 1-cell embryos for
231 microinjection. Melt 2% agarose in E3 (standard embryo medium) and pour into a Petri dish.
232 Carefully float the injection mold (see **Table of Materials**) on the top of the hot agarose to
233 generate the imprint of the troughs in the agarose as it solidifies. Once the agarose solidifies,
234 remove the injection mold.
235
236 NOTE: Injection mold dishes can be used for several months; cover in E3 and store at 4 °C when
237 not in use.
238
239 2.1.2. Pull microinjection needles. Pull glass capillaries to a long taper to make microinjection
240 needles using a needle puller machine. Program the machine specific to the type of capillaries
241 used. For 1.0 x 0.78 mm borosilicate capillaries use the following program: heat = 546 °C, pull =
242 130, velocity = 70, time = 90 (**Figure 2F**). Store the needles in a Petri dish and secure it with
243 modeling clay.
244
245 NOTE: The pulling recipe will vary, depending on the machine and filament, and new filaments
246 should always be calibrated. Each round of pulling produces two needles (**Figure 2G**); do this
247 several times to produce enough needles in case of accidental breaks and future experiments.
248
249 2.1.3. Dilute the capped RNA for injection. Dilute both EGFP-CAAX and H2A-mCherry RNAs to
250 200–300 ng/µL concentration using RNase-free H_2O and 1 µL of phenol red in a total volume of
251 5 µL (final concentration of phenol red is 0.1%). Flick the mixture and briefly spin down to collect
252 the total volume. Keep the diluted RNA on ice prior to injecting.
253
254 <mark>2.2. Injection of 1-cell embryos</mark>
255
256 <mark>2.2.1. Once the fish begin to breed, allow ~15–20 min to ensure that the eggs become fertilized.</mark>
257 <mark>During this time, backload the needle with 2.5–5 µL of the RNA dilution using a P10 and P10</mark>
258 <mark>micro-loader tips.</mark>
259
260 2.2.2. Using a picoinjector, calibrate the needle using an eyepiece reticle (a micrometer
261 calibration slide is also sufficient) to measure the volume of the droplet (volume of a sphere =

262   (4/3) * pi * radius^3). Adjust the injection time and pressure such that the injection volume is 1
263   nL (**Figure 2I**).

265   2.2.3. With a roller/transfer pipette, carefully load eggs into the injection mold (**Figure 2J**). If
266   helpful, use forceps to roll embryos such that the single cell is visible, either prior to or during
267   injection. It is the user's preference to use a micromanipulator.

269   2.2.4. Inject embryos at the 1-cell stage, targeting the cell and not the yolk (**Figure 2M**). This will
270   ensure uniform labeling of the developing embryo.

272   2.3. Raise embryos to the desired stage (prior to 12 hpf, according to standard staging[34]). Injected
273   embryos will have a delayed development, so raise them at a slightly higher temperature (29.0–
274   29.5 °C) to make up time. During the afternoon, check the embryos and remove those that are
275   dead to preserve the health of the clutch.

277   **3. Mounting optic vesicle stage zebrafish embryos for timelapse imaging**

279   3.1. Before mounting, prepare 1.6% low-melt agarose in E3. If planning multiple imaging
280   experiments, prepare ~20 mL of low-melt agarose and store at room temperature. On the day of
281   embryo mounting, melt this to generate a fresh aliquot (1–5 mL) in a tube that can be placed in
282   a 42 °C heat block prior to mounting.

284   3.2. Screen embryos for successful injection and overall brightness of fluorescence using a
285   fluorescence microscope prior to mounting. An ideal sample will have strong EGFP and mCherry
286   fluorescence and be at the correct developmental stage (**Figure 3B–B''**).

288   3.2.1. Screen embryos using a fluorescence microscope. Select embryos that strongly express
289   both EGFP and mCherry fluorescence for mounting.

291   3.2.2. Select embryos that are 11 hpf. Count somites to properly stage the embryos[34]; at 11 hpf
292   there should be 3 somites, and by 12 hpf there are 6 somites.

294   NOTE: By mounting embryos prior to 12 hpf (at 11 hpf), the samples will be appropriately staged
295   at 12 hpf when the timelapse begins.

297   3.3. Dechorionate embryos prior to mounting. Do this either manually with fine forceps or
298   chemically using pronase (2 mg/mL). With embryos this young, it is essential that dechorionation
299   is performed within an agar-coated dish and that embryos do not contact the air-water interface.

301   3.4. Using a glass roller pipette, suck up an embryo and eject as much E3 as possible such that
302   the embryo sits at the tip of the glass Pasteur pipette.
303

3.5. Drop the embryo into the tube of agarose from the heat block. Let it sink into the agarose for a few seconds, then suck up some agarose first and then the embryo, making sure that the embryo remains at the tip of the pipette (**Figure 3C–C'**).

3.6. Place a glass-bottom dish for imaging under a dissecting scope. Eject the embryo and agarose into an agarose droplet in the glass-bottom dish. Use forceps to very quickly orient, such that the embryo is dorsal-down (top of head on the glass bottom). Allow the agarose droplet to harden (**Figure 3D–D'**). This step must be done quickly but carefully, as embryos at this stage are fragile. Damaged embryos will not survive the timelapse imaging process.

NOTE: It is important to orient all embryos consistently for this experiment. When performing the timelapse, the embryos must fit within the assigned field of view while maintaining additional space for the optic vesicle to grow into. An optimal orientation is to align the anterior-posterior axis of all embryos "vertically" or along 12 and 6 on a clock face (**Figure 3G**).

3.7. Mount between 10–12 embryos, which is more than twice as many that will be imaged, so that the best samples can be selected once evaluated on the confocal (**Figure 3E–E'**). Samples will be evaluated for age, uniformity of fluorescent labeling, and precision of mounting orientation.

3.8. After mounting the embryos, pipette more agarose to completely cover the bottom of the dish, thereby encasing all of the separate agarose droplets in a single large agarose disc (**Figure 3F–F'**). A sufficient amount of agarose will ensure that the individual embryo droplets or the entire disc does not lift up from the bottom of the dish and float out of view.

3.9. Once hardened, overlay the agarose with E3 to keep the samples hydrated for the duration of the timelapse imaging experiment (a concern depending on the humidity of the building and in the environment).

NOTE: Tricaine is not necessary for these specific timelapse imaging experiments, as these embryos are sufficiently young; however, if desired, and if working with older stages of embryos, tricaine can be added into the agarose itself and overlaid in the media.

3.10. On paper, draw a map of the embryos for easy reference during timelapse set up. This is crucial to later associate the position with the genotype of each sample.

4. Multiple position confocal timelapse with a laser scanning confocal microscope

NOTE: This timelapse imaging protocol was designed to be used with a laser scanning confocal microscope equipped with manufacturer's software (see **Table of Materials**). This system is equipped with a piezo Z-stage device that allows rapid acquisition of Z-stacks. The laser lines used in this protocol are a 488 nm Argon ion laser and a DPSS 561 nm laser. The 561 nm laser is well-suited for imaging the mCherry fluorophore: it is close enough to the peak of mCherry excitation (587 nm) and well-powered.

348

349 **4.1. Set up the confocal.**

350

351 4.1.1. Power on the confocal and log into the desktop computer.

352

353 4.1.2. Install the piezo Z-stage insert (**Figure 4B**), then start the acquisition software.

354

355 4.1.3. In the software within **Acquisition** mode, turn on the 488 and 561 lasers using the drop-
356 down menu (**Figure 4F**). The lasers take several minutes to warm up, so this step is performed
357 early to save time.

358

359 NOTE: The acquisition parameters are as follows: Check the **Z-stack**, **Time Series**, and **Position**
360 boxes. Set **Frame Size** to 512 (X) x 384 (Y), **Scan Speed** to 9, **Scan Mode** to bidirectional, **Zoom** to
361 0.7, **Pinhole** to 60.2 (1.63 Airy Units ~= 1.6 μm section), and **Z-interval** to 2.1 μm. This will yield
362 an image size of 303.6 μm x 227.7 μm, and pixel size of 0.59 μm. The 488 and 561 lasers should
363 be checked and assigned to the same track; the EGFP detection range is 494–545 nm and the
364 mCherry detection range is 598–679 (**Figure 4F**).

365

366 4.1.4. Liberally coat the bottom of the glass dish with immersion medium matching the refractive
367 index of water, being careful to avoid air bubbles (**Figure 4C**). Select the 40x water objective and
368 apply a small drop of immersion medium to the objective (**Figure 4D**). Secure the glass-bottomed
369 dish in the stage insert, apply E3 to keep the embryos moist overnight, then use modeling clay to
370 seal the plastic lid over the dish (**Figure 4E**). Raise the objective to make contact with the dish.

371

372 **4.2. Screen samples and prepare for timelapse.**

373

374 4.2.1. Switch from the **Acquisition** tab to the **Locate** tab and click on the lightbulb symbol to turn
375 on transmitted light. With the transmitted light, locate the first sample with the joystick: by eye,
376 first move the sample into the beam of light, then use the eyepieces to the center and focus on
377 an optic vesicle.

378

379 4.2.2. Return to the **Acquisition** tab. Ensure that the **Z-stack**, **Time Series**, and **Positions** boxes
380 are checked, and the lasers are warmed up for use.

381

382 4.2.3. Set the **Frame Size** to 512 (X) x 384 (Y), **Scan Speed** to 9, **Scan Mode** to bidirectional, and
383 set **Zoom** to 0.7.

384

385 4.2.4. Under the **Channels** heading, begin by assigning the 488 and 561 lasers to **Power** 2.0 and
386 **Gain** 550 (this can be adjusted later). Set the **pinhole** to 60.2 (1.63 Airy Units ~= 1.6 μm section).

387

388 4.2.5. Begin scanning using the **Continuous** button. With the fine focus knob, locate the sample
389 in the Z-axis and position the X-Y axis in frame. Stop scanning.

390

4.2.6. Under the **Positions** heading, click on **Add** to save the XYZ information on the first sample (**Figure 4F**). Do this only for samples to be timelapsed. Select samples for their strong fluorescence and optimal mounting.

4.2.7. Switch to the **Locate** tab, move to the next sample, and repeat steps 4.2.5–4.2.6, being selective about choosing samples.

4.3. Finalize sample positions, assign z-range, and then start timelapse. Once all the samples are selected (it is possible to image 4–5 samples within the 2.5-minute total time interval) and positions are saved, go through each sample and adjust the XYZ position within the viewing frame.

4.3.1. Highlight the first position and click on **Move To**. While continuously scanning, line up the optic vesicle within the frame. Leave ample space in the anterior and distal regions relative to the optic vesicle and the brain.

4.3.2. Next, assign the first and last Z-slices by selecting **Set First** and **Set Last** while moving through the Z-direction with the fine focus knob. Maintain a total slice number of ~63, as this will accommodate the growth of the optic cup. Provide extra room on the ventral side of the optic vesicle to allow room for growth.

4.3.3. Once first and last Z-slices have been set, click on the **C** button to move to the center of the Z-stack. Adjust laser power and gain for both lasers; if possible, keep the laser power below 5 and use a higher gain, if necessary. Stop Scanning. Update the position information by clicking on **Update**.

4.3.4. Move to the next position by clicking on **Position 2**. Repeat steps 4.3.1–4.3.3 for each assigned position. The laser power and gain should be set such that all samples are sufficiently illuminated.

4.3.5. Once both position information and laser settings are finalized, assign **Time Series** settings. Under the Time Series heading, assign **Time Interval** to 2.5 min, and **Cycles to 300** (**Figure 4F**). The number of cycles is calculated such that the timelapse proceeds past the 24 hpf stage, when optic cup development is complete.

4.3.6. To begin the timelapse, click on **Start**. Monitor the first complete cycle: use a timer to ensure one complete cycle (imaging all positions) is less than 2.5 min and verify that each position looks correct. The microscope runs independently overnight and does not need to be monitored.

NOTE: Although the confocal room is temperature controlled, the room temperature is 20–25 °C. With the equipment running and the lasers scanning, the temperature on the stage appears to be closer to 28.5 °C, since embryonic development proceeds at this expected rate, as assayed visually with morphological landmarks.

435   4.3.7. With these settings, the timelapse will last 12.5 h. Save the file once the timelapse is
436   complete. It will be large (~40 GB) and can be separated into individual positions after it is saved
437   using the acquisition software.
438
439   **REPRESENTATIVE RESULTS:**
440
441   **Injection of fluorescent RNAs enables subcellular labeling**
442
443   RNAs that label the cell's plasma membrane and histones are injected in order to capture the
444   individual cell morphologies and movements that underlie optic cup morphogenesis. **Figure 2**
445   demonstrates each step of the process of microinjecting zebrafish embryos at the 1-cell stage.
446   Briefly, zebrafish are mated (**Figure 2E**), and embryos are collected and loaded into the
447   injection mold (**Figure 2J**). A microinjection needle is backfilled (**Figure 2H**), and embryos are
448   injected directly into the single cell (**Figure 2K–M**), which is necessary to obtain uniform
449   labeling (**Figure 2M, Figure 4I–I''', Movie 1**). In addition to uniform labeling, robust
450   fluorescence is observed and development proceeds unperturbed (**Figure 3B–B''**).
451
452   **Effective mounting is essential for timelapse imaging OCM from 12–24 hpf**
453
454   To image optic cup morphogenesis, which occurs over an extended period of time, it is critical
455   to both select ideal embryos and properly position each sample while embedding. **Figure 3**
456   shows a detailed account for successful mounting of 11 hpf embryos. Injected embryos are first
457   screened for sufficient fluorescence (**Figure 3B',B'',F'',F'''**). Individual embryos are immersed in
458   agarose (**Figure 3C,C'**) and mounted dorsally in an individual drop of agarose (**Figure 3D,D'**). All
459   samples are mounted in a collective disc of agarose (**Figure 3E–F'**). When embryos are staged
460   correctly, sufficiently fluorescent, and adequately mounted (**Figure 3G**), the samples will stay in
461   the imaging frame during the timelapse allowing for the entire organ to be imaged (**Figure 4G–**
462   **G'', I–I''', Movie 1**). Failure to accomplish any of these steps will result in a mounted embryo
463   that is not an optimal sample for timelapse imaging. The slightest variation in the degree of
464   rotation will have a dramatic effect on the direction of embryo growth during the timelapse.
465   Sub-optimal rotations are shown in **Figure 3**, including an embryo that is over-rotated (**Figure**
466   **3I**), which will result in a more posterior timelapse, and an embryo that is under-rotated (**Figure**
467   **3J**) in which only the most anterior tissue can be observed. In addition to proper rotation during
468   mounting, samples that are mounted with respect to the orientation of the frame are more
469   likely to yield a successful timelapse (**Figure 4G–G'', I–I''', Movie 1**). Optimal samples are those
470   that are oriented vertically on the dish, with the anterior-posterior axis in line with 12 and 6 on
471   a clock face (**Figure 3G**). Sub-optimal samples are those that are not oriented on this axis, such
472   as those that are horizontal or diagonal (**Figure 3H**). These samples will grow out of the imaging
473   frame as the timelapse proceeds and cannot be used for further analysis (**Figure 4H–H'', J–J'''**).
474
475   **Acquiring a timelapse dataset that is suitable for future analysis**
476
477   Embryos that are accurately injected, raised, and mounted will make for successful confocal
478   imaged samples. **Figure 4** shows an optimal sample for timelapse: there is even fluorescence, and

479 the sample is 12 hpf. The z-stack for imaging is assigned such that the first slice is just dorsal to
480 the optic vesicle, while the last slice leaves several slices beyond the ventral boundary of the 12
481 hpf optic vesicle (**Figure 4G–G''**). This bias toward the ventral side provides excess space for tissue
482 growth in the ventral direction. These factors, when met, result in an optimal timelapse (**Figure
483 4I–I''', Movie 1**). A sub-optimal sample has mosaic or dim fluorescence, has already developed
484 past 12 hpf (when optic cup morphogenesis is under way), or is positioned poorly in the Z-stack
485 or the XY frame (**Figure 4H–H''**). When these criteria are not met, the timelapse will no longer
486 capture the entire 3D volume of the tissue as it develops and cannot be used for further analysis
487 (**Figure 4J–J'''**).

489 **FIGURE AND TABLE LEGENDS:**

491 **Figure 1: Workflow of 4D timelapse imaging of zebrafish optic cup morphogenesis.** (**A**) To
492 fluorescently label subcellular structures of interest, synthesize the appropriate capped mRNAs.
493 (**B**) Microinject mRNA(s) into zebrafish embryos at the 1-cell stage. (**C**) Embryos are mounted
494 dorsally, or head-down for an inverted confocal microscope, at the optic vesicle stage, ~11 h post
495 fertilization or 3 somite-stage. (**D**) Multiple embryos can be sequentially imaged during a single
496 timelapse imaging session.

498 **Figure 2: A visual guide for microinjecting 1-cell zebrafish embryos.** (**A**) Items to include in an
499 injection kit (clockwise): medium sized box that can hold the entire kit with disposable nitrile
500 gloves; a dish containing microinjection needles; forceps; an aliquot of mineral oil and cut up
501 squares of parafilm; microloading tips; diluted RNA on ice; agarose injection mold; marker;
502 roller/transfer pipette; and P10 pipette. (**B**) Microinjection set-up: a dissecting microscope next
503 to a pico-injector that is connected to an external compressed gas source. A foot pedal and
504 micromanipulator are attached to the pico-injector. The micromanipulator is equipped with a
505 needle holder and positioned in place above the microscope stage. (**C**) An agarose injection mold
506 containing six rows of grooves with a 90-degree angle on one side and a 45-degree angle on the
507 other side. (**D**) The pico-injector front panel. The pressure display reads 7.8 PSI; this can be
508 adjusted with the knob labeled P_{inject}. Beneath, there are pushbuttons to manually trigger
509 pressure to inject, to change the injection time, or to clear, fill, or hold the liquid in the needle.
510 The inject time is set to 08 (equivalent to 8 x 10 msec). An output hose is connected to P_{out} and
511 is attached to the injection needle. The pressure meter source switch is set to P_{inject} while setting
512 the injection pressure, and it can be switched to $P_{balance}$ to adjust the basal pressure applied to
513 the needle when injections are not being made. The $P_{balance}$ regulator is next to the P_{inject}
514 regulator. The power button is lit to indicate the machine is turned on. (**E**) Adult zebrafish are
515 mated in small breeding tanks that contain a nested tank with a mesh bottom that separates
516 adult fish from fertilized eggs and allows easy collection. Water level is lowered to mimic shallow
517 water conditions and tank dividers are removed to initiate mating behavior. (**F**) The micropipette
518 (needle) puller front panel: contains a display which shows the specific conditions used to pull
519 needles. The pressure setting is P = 500, followed by the last date and time the program was
520 edited, the program number, HEAT = 546, PULL = 130, VEL = 70, and TIME = 90. (**G**) One glass
521 capillary is inserted into the micropipette (needle) puller and secured into place. Each
522 programmed pull run results in two long tapered needles (red arrowheads). (**H**) The RNA dilution

is backloaded into a needle; the phenol red dye allows easy visualization of the solution. (**I**) After breaking the tip of the needle, the bolus of RNA is measured using an eyepiece reticle on the dissecting scope. For this stereomicroscope, at 30x total magnification 6 hash marks is equal to 1 nL volume. (**J**) Fertilized eggs are loaded into the agarose injection mold and distributed along the troughs of the mold using a roller pipette. (**K**) The injection mold containing one-cell stage embryos is positioned under the microscope and embryos are injected sequentially. (**L**) The injection needle is inserted into each embryo targeting the single cell. (**M**) Once in the cell, the foot pedal is used to trigger a regulated amount of pressure and the release of 1 nL of RNA into the cell of the embryo (as visualized by phenol red). Scale bars: I = 0.1 mm; L, M = 0.5 mm.

Figure 3: A visual guide for mounting embryos for imaging. (**A**) Mounting set up (from left to right): a heat block programmed to 42 °C, heating tubes of low-melt agarose; a roller pipette; a pair of forceps; an agarose coated dish containing dechorionated embryos; and a dissecting stereomicroscope connected to a metal halide fluorescent lamp. (**B,B',B''**) An 11 hpf embryo injected with EGFP-CAAX mRNA and mCherry-H2A mRNA, shown under brightfield, GFP fluorescence and mCherry fluorescence, respectively. (**C,C'**) A glass pasteur pipette containing agarose and an embryo sitting in the tip; **C'** is a magnified view. (**D,D'**) One embryo mounted in a droplet of low-melt agarose on a glass bottomed dish, seen both from the stage of the microscope and through the microscope eyepieces. (**E,E'**) 12 embryos mounted in individual droplets of low-melt agarose on a glass bottomed dish, seen both from the stage of the microscope and through the microscope eyepieces. (**F,F',F'',F'''**) All mounted embryos are overlaid with a complete layer of agarose to fill the bottom of the dish, seen both from the stage of the microscope and from the microscope eyepieces shown in bright field; **F''** GFP fluorescence; and **F'''** mCherry fluorescence. (**G**) An optimal sample at 12 hpf is mounted dorsally and oriented vertically in line with 12 and 6 o'clock with both optic vesicles in the same plane. (**H**) A sub-optimal sample: although mounted dorsally and optic vesicles are in plane with each other, this sample is oriented on a diagonal axis and will grow out of the frame size as development proceeds. (**I**) A sub-optimal sample: this sample is over-rotated and not a dorsal mount, as a result, the anterior portion of the optic vesicle will not be captured in the timelapse. (**J**) A sub-optimal sample: this sample is under-rotated and not a dorsal mount, as a result the posterior portion of the optic vesicle will not be captured in the timelapse. Dotted lines indicate each optic vesicle. Scale bars: B = 0.1 mm; D' = 1.5 mm; E', F' = 2.5 mm; G = 0.1 mm.

Figure 4: Setting up a multiple position timelapse and potential results. (**A**) Laser scanning confocal microscope. (**B**) Piezo Z-stage insert. (**C**) The bottom of a glass bottom dish containing embryos embedded in agarose is coated in immersion medium matching the refractive index of water. (**D**) A droplet of immersion medium is placed on the 40x W objective (long working distance). (**E**) The dish is held into place with the stage insert, E3 is added on top of the agarose layer, and the lid is secured with modeling clay. (**F**) Acquisition software settings: The desired laser lines are turned on from the drop-down menu. For embryos injected with EGFP-CAAX RNA and H2A-mCherry RNA, the Argon and DPSS 561-10 lasers are turned on. The red highlight indicates that the Argon laser is warming up. To locate the sample over the objective, the transmitted light is turned on through the microscope control panel. Both EGFP and mCherry are assigned to Track 1 (for simultaneous imaging) and the range of each detector is set. Here, the

EGFP range is set to 494–545 nm, and the mCherry range is set to 598–679 nm. Under the **Channels** menu, laser power can be set. After the lasers have warmed up, the power can be increased up to 5.0, and gain (master) can be adjusted. The pinhole is set at 60.2, which is equal to 1.63 Airy Units or 1.6 μm section. Under the Acquisition menu, the frame size is set to 512 x 384, scan speed is 9.0, averaging is bidirectional, and zoom is set to 0.7. Under the Z-Stack menu, the first and last position in the Z-axis are set while the confocal is scanning. The interval (step size) is set to 2.1 μm. While choosing first and last Z-position, a standard number of 63 slices is generally maintained; this accommodates the overall growth of the eye. The "use piezo" option is selected. Under the **Positions** menu, each selected position is listed including an assigned number and X, Y, and Z position. There are additional buttons to control the number of embryos (separate positions) to image, including add, update, or remove. Under the **Time Series** menu, the cycle is set to 300 (the number of Z-stacks that will be acquired) and interval (time step) is set to 2.5 min. Once the settings are finalized, timelapse acquisition is initiated by pressing start. The software will show the slice of the Z-stack, the cycle, and the position that is currently scanning. When the timelapse is complete, the file is saved by clicking on the floppy disk icon in the **Images and Documents** panel. (**G–J**) Cell membranes (*green*) are labeled with EGFP-CAAX and cell nuclei (chromatin, *magenta*) are labeled with H2A-mCherry RNAs. (**G,G',G''**) An example of setting the first and last Z-slice for an optimally mounted sample. The first Z-slice (at the dorsal side) comes at the expense of dorsal ectoderm, while the last Z-slice (at the ventral side) is well below the optic vesicle, to accommodate its growth in the ventral direction. (**H,H',H''**) An example of setting the first and last Z-slice of a sub-optimal sample. The sample has weak mCherry fluorescence and it is mounted diagonally, such that the developing optic cup is unlikely to stay in frame for the duration of the timelapse. (**I,I',I'',I'''**) An example of a timelapse from an optimal sample. Single slice images from the middle of the Z-stack are taken from the entire 63 slice volume at 4 time points (T value). Br, brain; NR, neural retina; RPE, retinal pigmented epithelium; Le, lens. (**J,J',J'',J'''**) An example of a timelapse from a suboptimal sample. In this case, the sample moved out of the Z-plane and only an oblique portion of the anterior optic cup was captured. Scale bars: G, I = 50 μm.

Movie 1: Timelapse of optic cup morphogenesis in an optimal wild type embryo. A dorsal view of a wild type embryo that is labeled with EGFP-CAAX (plasma membranes, *green*) and H2A.F/Z-mCherry (chromatin, *magenta*). The timelapse is from ~12–24 hpf and contains a single confocal section from an entire 4D dataset. Time interval is 2.5 min between z-stacks and is shown at 22.5 frames per second.

DISCUSSION:
Here, we describe a protocol for in toto labeling and 4D timelapse imaging of optic cup morphogenesis. We step through the process of generating capped RNA encoding fluorescent proteins to mark different subcellular compartments; injecting zebrafish 1-cell embryos; embedding 11 hpf embryos in agarose for multiplexed imaging; and acquiring 4D datasets of multiple embryos for the duration of optic cup morphogenesis (12–24 hpf).

A myriad of questions can be answered with these information-dense datasets. 4D data can be visualized and quantitatively analyzed in a variety of ways. Although outside of the scope of this

611   protocol, we include here some of our goals and standard applications as an example of the types
612   of things that can be accomplished. Of course, quantitative image analysis methods are
613   constantly being developed, and both commercially available and custom-built tools can be used.
614   If one has not used such methods before, one should be prepared to work through some
615   optimization to ensure that the acquired datasets are adequate for the quantitative analysis
616   approach of choice.
617
618   Visualizing and quantitatively evaluating the 4D datasets can be challenging, due to the size of
619   the files. The acquisition software can be used to separate the datasets into individual embryos,
620   and ImageJ/Fiji can be used to convert confocal files from commercial formats to more standard
621   tif stacks, in which each timepoint is saved as a separate file. This will decrease the file sizes and
622   standardize the file formats. Individual optical sections from each timepoint can be assembled as
623   a 2D (XY) timelapse using ImageJ/Fiji, enabling rapid 2D visualization and evaluation of the data.
624   **Movie 1** is an example of precisely this: a single optical section over time assembled as a
625   timelapse of the optimal sample shown in **Figure 4I–I'''**. From there, for 3D and 4D visualization,
626   we commonly use FluoRender[35,36], which is freely available but has specific graphics card
627   requirements. Using FluoRender, one can rotate 3D-rendered data in any axis, visualize the
628   dataset in 4D over time, generate cutaways in any plane, and save the rotations and visualizations
629   as a movie or series of tif images.
630
631   In terms of quantitative analysis, there are numerous questions to be answered. We have
632   developed software in-house to aid our own specific goals of understanding the cell behaviors
633   underlying optic cup morphogenesis. Our program, LongTracker, uses the nuclear signal as a
634   proxy for position to track cells[13]. With these data, we can determine when, where, and how cells
635   move; how fast and how far cells move; and how frequently cells divide. In addition to our own
636   software, there are multiple commercially available and custom-built options for 4D cell tracking.
637   We have also developed the program LongAxis to carry out cell segmentation and quantify cell
638   shape and organization within the neural retina[37]. The datasets input into LongAxis, however, are
639   single Z-stacks, taken at a high resolution. A persistent challenge has been generating timelapse
640   datasets with high enough resolution that cells can be segmented with confidence and their
641   morphology extrapolated. One alternative is mosaic (sparse) labeling using a photoconvertible
642   fluorophore such as Kaede for direct visualization of cell shape, as we and others have carried
643   out in the developing eye[8,11,13]. This simplifies the cell segmentation problem, and cell shape and
644   size can be readily quantified through 3D rendering in FluoRender.
645
646   Each step of this protocol was optimized specifically for our purposes. The specificity of this
647   protocol results in several limitations: the protocol, as written, is not optimized for imaging other
648   aspects of zebrafish eye development (such as retinal neurogenesis), other eye structures, other
649   developmental stages, or other subcellular compartments. The orientation of embedding, the
650   speed of imaging, and the labels are all designed to allow us to answer our biological questions.
651   In order to image retinal neurogenesis, for example, the dorsal orientation of the embryo as
652   described here may not allow for visualization of specific features of interest, and the speed of
653   imaging may not be appropriate. Many aspects of the protocol can be adapted and modified for
654   a variety of needs, depending on one's specific interests and goals. First, using RNA injections

makes the labeling process very flexible. Fluorescent protein fusion constructs can be used to label subcellular structures of interest, and RNA injection amount can be varied to optimize labeling. Based on our work with the photoconvertible fluorophore Kaede, RNA injections appear to support a burst of translation that is over by 12 hpf[11,13]. High levels of fluorescent protein expression from RNA injection could combat photobleaching, but such an approach does not support sustained expression of the fluorescent label of interest. If sustained expression is necessary, such as when imaging embryos at later stages, transgenic lines are an option, and constructing new lines in zebrafish is straightforward[24].

Next, the protocol can be adapted for later stages of development. Because pigment may impede imaging at later stages, embryos can be treated with phenylthiourea (PTU) to inhibit pigment formation, or genetic mutants for pigment synthesis can be used. To prevent embryo twitching, tricaine can be added to the agarose and embryo media overlay solutions, and the percent agarose can be adjusted as necessary. As the eye grows, it may be necessary to change the mounting orientation; here, we mount embryos dorsally, but at later stages, it may make more sense to mount laterally or anteriorly, depending on the structure of interest. Because different processes occur over different spatial and temporal scales, one can also optimize the Z-step and time step of image acquisition. These features can really only be determined empirically for each lab's needs.

Finally, this protocol was developed specifically for a laser scanning confocal microscope, with embryos embedded in a relatively high percentage of agarose at an early stage of eye development. If one is imaging at different times or different locations during eye development, this protocol will need to be adapted for the process of interest. Many different imaging approaches are currently possible, with more being developed by optical engineers. Each approach brings its own set of challenges, from different ways to embed and mount embryos for imaging, to different file sizes and formats. We outline considerations in the introduction to guide the optimization process, in which maximal spatial and temporal resolution are balanced with photobleaching, phototoxicity, and immense file sizes. We hope that these general principles, in addition to the practical information described above, will aid others in establishing timelapse imaging approaches to study the many open questions in eye development.

DISCLOSURES:
The authors have nothing to disclose.

REFERENCES:

1.   Adler, R., Canto-Soler, M. V. Molecular mechanisms of optic vesicle development: complexities, ambiguities and controversies. *Developmental Biology*. **305** (1), 1–13 (2007).

699   2.   Chow, R. L., Lang, R. A. Early eye development in vertebrates. *Annual Review of Cell and*
700   *Developmental Biology*. **17**, 255–296 (2001).
701   3.   Fuhrmann, S. Eye morphogenesis and patterning of the optic vesicle. *Current Topics in*
702   *Developmental Biology*. **93**, 61–84 (2010).
703   4.   Martinez-Morales, J. R., Wittbrodt, J. Shaping the vertebrate eye. *Current Opinion in*
704   *Genetics and Development*. **19** (5), 511–517 (2009).
705   5.   Yang, X. J. Roles of cell-extrinsic growth factors in vertebrate eye pattern formation and
706   retinogenesis. *Seminars in Cell & Developmental Biology*. **15** (1), 91–103 (2004).
707   6.   Bogdanovic, O. et al. Numb/Numbl-Opo antagonism controls retinal epithelium
708   morphogenesis by regulating integrin endocytosis. *Developmental Cell*. **23** (4), 782–795 (2012).
709   7.   Bryan, C. D., Casey, M. A., Pfeiffer, R. L., Jones, B. W., Kwan, K. M. Optic cup
710   morphogenesis requires neural crest-mediated basement membrane assembly. *Development*.
711   **147** (4) (2020).
712   8.   Bryan, C. D., Chien, C. B., Kwan, K. M. Loss of laminin alpha 1 results in multiple structural
713   defects and divergent effects on adhesion during vertebrate optic cup morphogenesis.
714   *Developmental Biology*. **416** (2), 324–337 (2016).
715   9.   Cavodeassi, F., Ivanovitch, K., Wilson, S. W. Eph/Ephrin signalling maintains eye field
716   segregation from adjacent neural plate territories during forebrain morphogenesis.
717   *Development*. **140** (20), 4193–4202 (2013).
718   10.   England, S. J., Blanchard, G. B., Mahadevan, L., Adams, R. J. A dynamic fate map of the
719   forebrain shows how vertebrate eyes form and explains two causes of cyclopia. *Development*.
720   **133** (23), 4613–4617 (2006).
721   11.   Gordon, H. B. et al. Hedgehog signaling regulates cell motility and optic fissure and stalk
722   formation during vertebrate eye morphogenesis. *Development*. **145** (22) (2018).
723   12.   Ivanovitch, K., Cavodeassi, F., Wilson, S. W. Precocious acquisition of neuroepithelial
724   character in the eye field underlies the onset of eye morphogenesis. *Developmental Cell*. **27** (3),
725   293–305 (2013).
726   13.   Kwan, K. M. et al. A complex choreography of cell movements shapes the vertebrate eye.
727   *Development*. **139** (2), 359–372 (2012).
728   14.   Martinez-Morales, J. R. et al. Ojoplano-mediated basal constriction is essential for optic
729   cup morphogenesis. *Development*. **136** (13), 2165–2175 (2009).
730   15.   Miesfeld, J. B. et al. Yap and Taz regulate retinal pigment epithelial cell fate. *Development*.
731   **142** (17), 3021–3032 (2015).
732   16.   Nicolas-Perez, M. et al. Analysis of cellular behavior and cytoskeletal dynamics reveal a
733   constriction mechanism driving optic cup morphogenesis. *eLife*. **5** (2016).
734   17.   Picker, A. et al. Dynamic coupling of pattern formation and morphogenesis in the
735   developing vertebrate retina. *PLoS Biology*. **7** (10), e1000214 (2009).
736   18.   Rembold, M., Loosli, F., Adams, R. J.,Wittbrodt, J. Individual cell migration serves as the
737   driving force for optic vesicle evagination. *Science*. **313** (5790), 1130–1134 (2006).
738   19.   Sidhaye, J., Norden, C. Concerted action of neuroepithelial basal shrinkage and active
739   epithelial migration ensures efficient optic cup morphogenesis. *eLife*. **6** (2017).
740   20.   Driever, W. et al. A genetic screen for mutations affecting embryogenesis in zebrafish.
741   *Development*. **123**, 37–46 (1996).

742   21.   Haffter, P. et al. The identification of genes with unique and essential functions in the
743   development of the zebrafish, Danio rerio. *Development*. **123**, 1–36 (1996).
744   22.   Nusslein-Volhard, C. The zebrafish issue of Development. *Development*. **139** (22), 4099–
745   4103 (2012).
746   23.   Hoshijima, K. et al. Highly efficient CRISPR-Cas9-based methods for generating deletion
747   mutations and F0 embryos that lack gene function in zebrafish. *Developmental Cell*. **51** (5), 645–
748   657, e644 (2019).
749   24.   Kwan, K. M. et al. The Tol2kit: a multisite gateway-based construction kit for Tol2
750   transposon transgenesis constructs. *Developmental Dynamics*. **236** (11), 3088–3099 (2007).
751   25.   Almeida, A. D. et al. Spectrum of Fates: a new approach to the study of the developing
752   zebrafish retina. *Development*. **141** (9), 1971–1980 (2014).
753   26.   Baye, L. M., Link, B. A. Interkinetic nuclear migration and the selection of neurogenic cell
754   divisions during vertebrate retinogenesis. *The Journal of Neuroscience*. **27** (38), 10143–10152
755   (2007).
756   27.   Clark, B. S. et al. Loss of Llgl1 in retinal neuroepithelia reveals links between apical domain
757   size, Notch activity and neurogenesis. *Development*. **139** (9), 1599–1610 (2012).
758   28.   Das, T., Payer, B., Cayouette, M., Harris, W. A. In vivo time-lapse imaging of cell divisions
759   during neurogenesis in the developing zebrafish retina. *Neuron*. **37** (4), 597–609 (2003).
760   29.   Kay, J. N. et al. Transient requirement for ganglion cells during assembly of retinal synaptic
761   layers. *Development*. **131** (6), 1331–1342 (2004).
762   30.   Norden, C., Young, S., Link, B. A., Harris, W. A. Actomyosin is the main driver of interkinetic
763   nuclear migration in the retina. *Cell*. **138** (6), 1195–1208 (2009).
764   31.   Suzuki, S. C. et al. Cone photoreceptor types in zebrafish are generated by symmetric
765   terminal divisions of dedicated precursors. *Proceedings of the National Academy of Sciences of
766   the United States of America*. **110** (37), 15109–15114 (2013).
767   32.   Wan, Y. et al. The ciliary marginal zone of the zebrafish retina: clonal and time-lapse
768   analysis of a continuously growing tissue. *Development*. **143** (7), 1099–1107 (2016).
769   33.   Yoshimatsu, T. et al. Presynaptic partner selection during retinal circuit reassembly varies
770   with timing of neuronal regeneration in vivo. *Nature Communications*. **7**, 10590 (2016).
771   34.   Kimmel, C. B., Ballard, W. W., Kimmel, S. R., Ullmann, B., Schilling, T. F. Stages of
772   embryonic development of the zebrafish. *Developmental Dynamics*. **203** (3), 253-310 (1995).
773   35.   Wan, Y., Otsuna, H., Chien, C. B., Hansen, C. An interactive visualization tool for multi-
774   channel confocal microscopy data in neurobiology research. *IEEE Transactions on Visualization
775   and Computer Graphics*. **15** (6), 1489–1496 (2009).
776   36.   Wan, Y., Otsuna, H., Chien, C. B., Hansen, C. FluoRender: an application of 2D image space
777   methods for 3D and 4D confocal microscopy data visualization in neurobiology research. *IEEE
778   Pacific Visualization Symposium*. 201–208 (2012).
779   37.   Carney, K. R., Bryan, C. D., Gordon, H. B., Kwan, K. M. LongAxis: a MATLAB-based program
780   for 3D quantitative analysis of epithelial cell shape and orientation. *Developmental Biology*. **458**
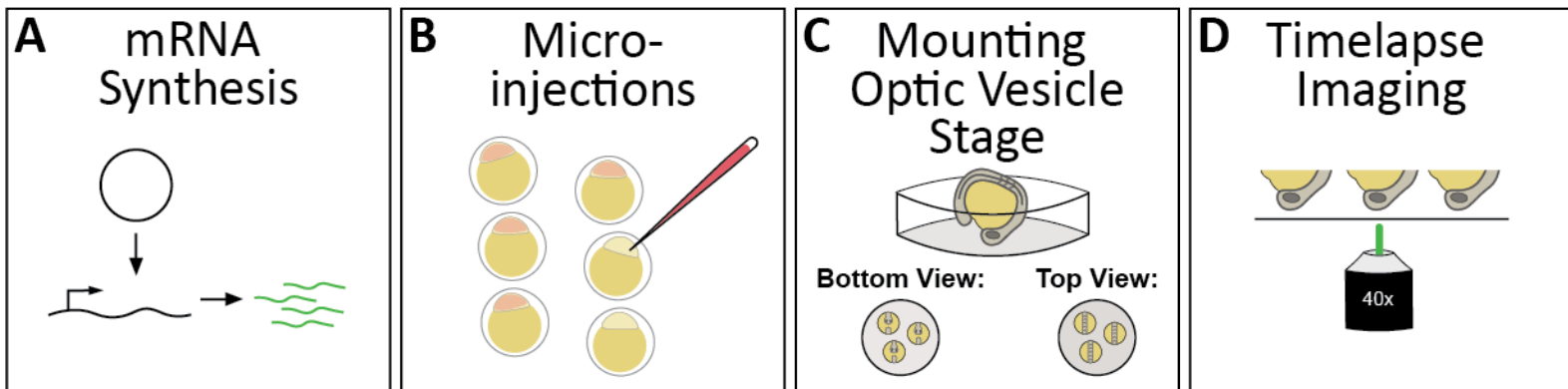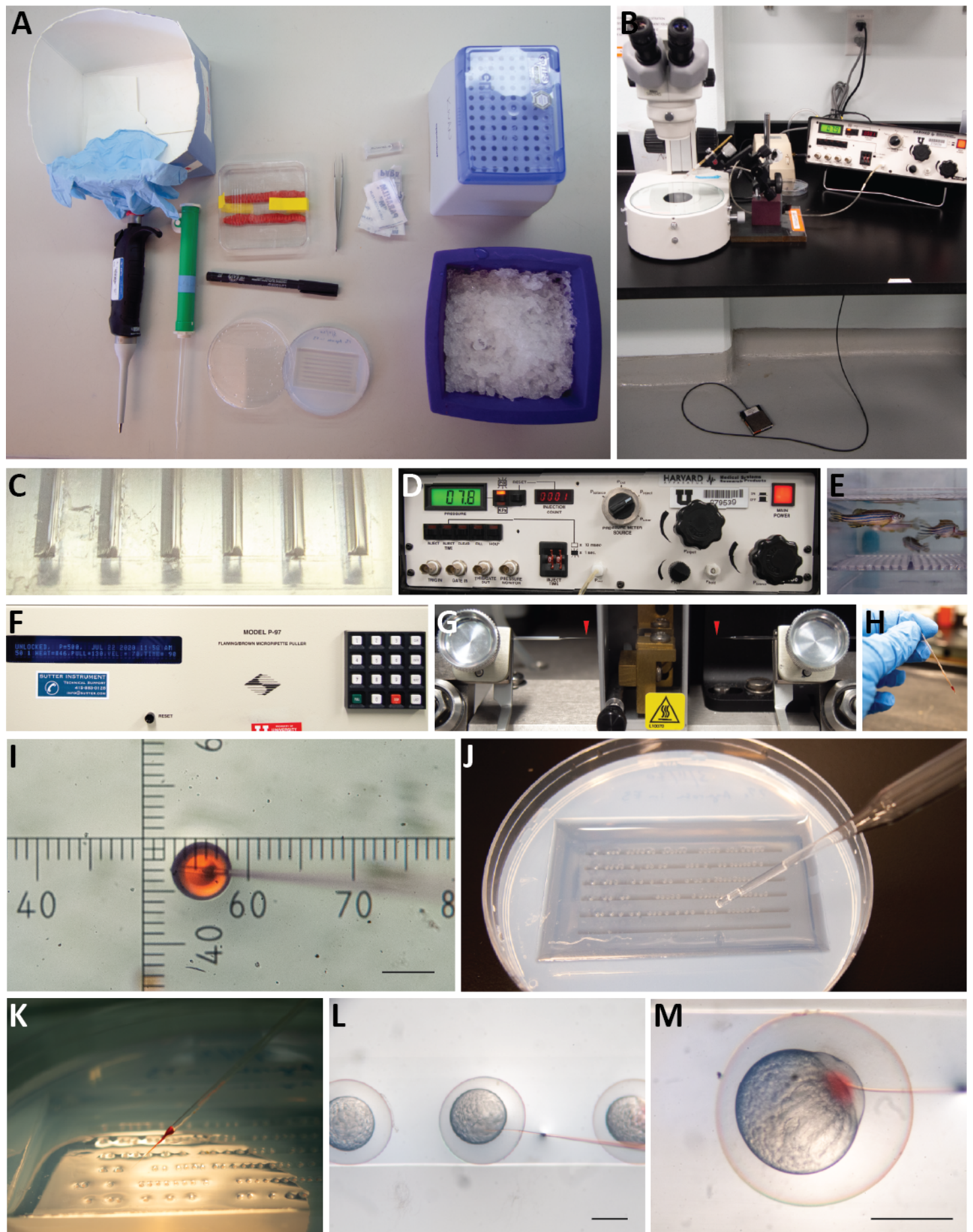781   (1), 1–11 (2020).
782

Figure 1

Figure 1
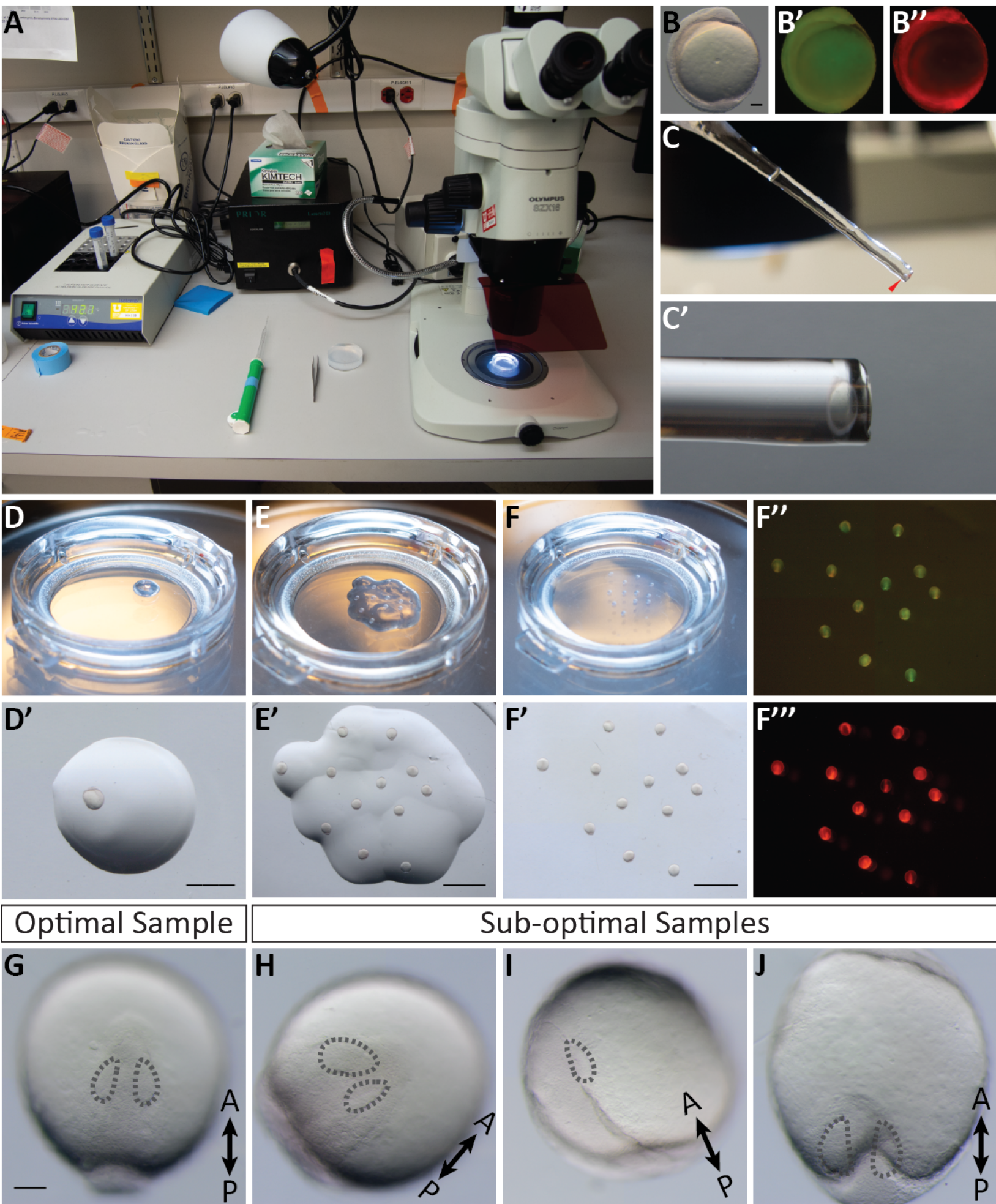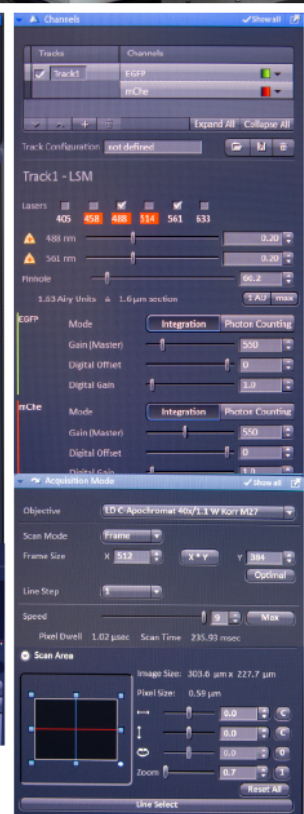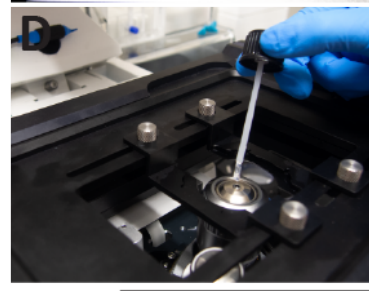
Figure 2

Click here to access/download;Figure;Figure2.pdf ⬇

Figure 2

Figure 3

Figure 3

Optimal Sample

Sub-optimal Samples

Figure 4

Figure 4

A

B

C

D

E

F

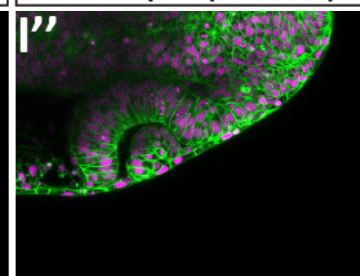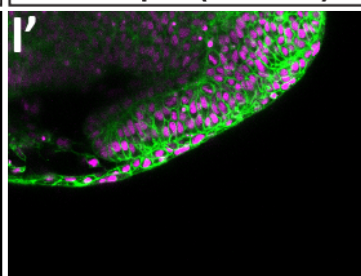| Optimal Sample	Sub-optimal Sample
G set last	**H**
G' center	**H'**
G'' set first	**H''**
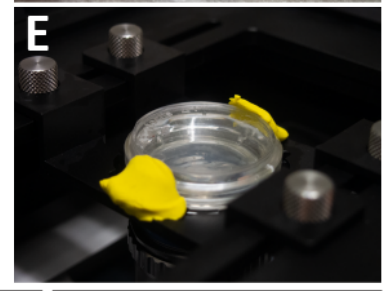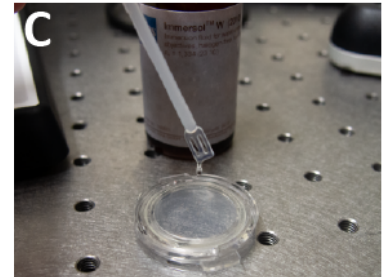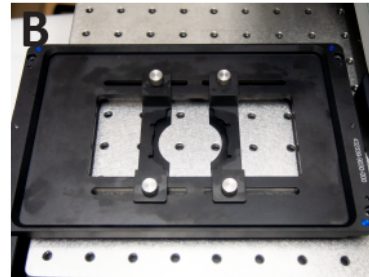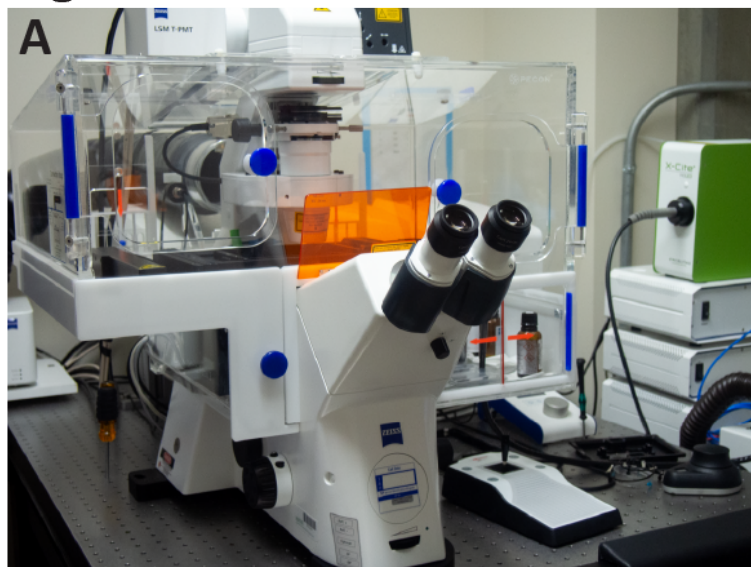
EGFP-CAAX, H2A.F/Z-mCherry
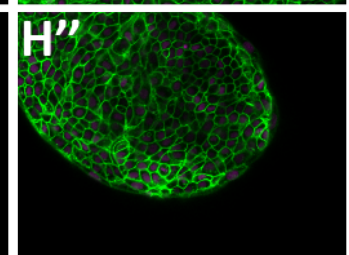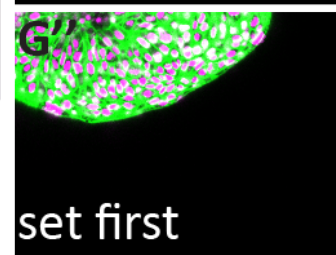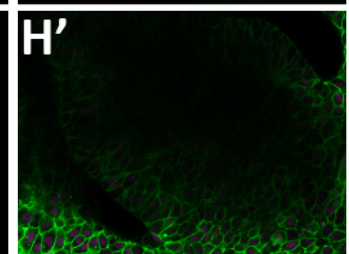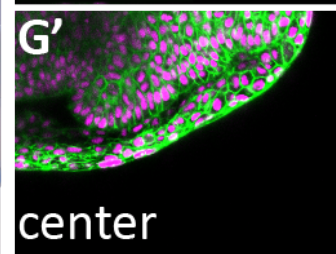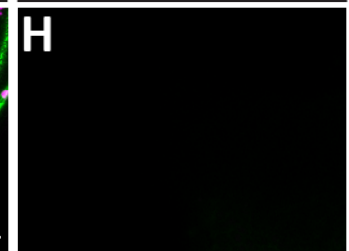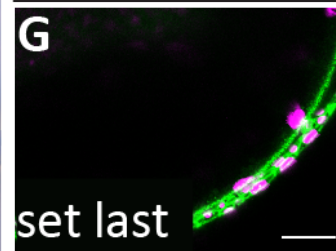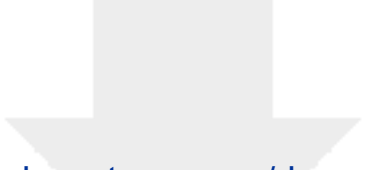
	12 hpf (T001)	16 hpf (T097)	20 hpf (T193)	24 hpf (T289)
Optimal Sample	**I**	**I'**	**I''**	**I'''**
Sub-optimal Sample	**J**	**J'**	**J''**	**J'''**
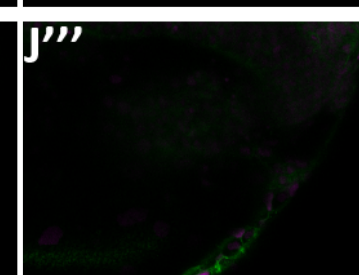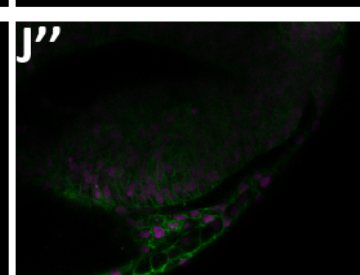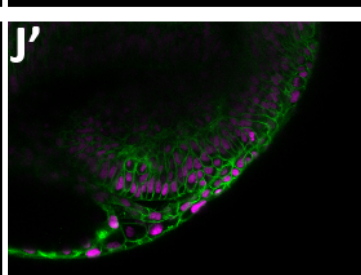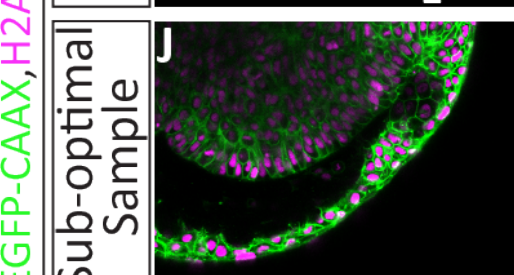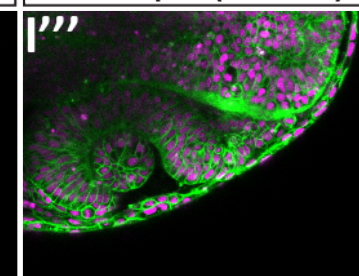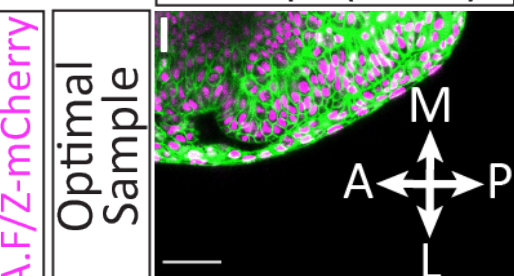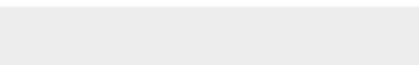
Movie 1

Click here to access/download
Video or Animated Figure
Movie1.mov

Name of Material/ Equipment	Company	Catalog Number	Comments/Description
Delta TPG Dish 0.17mm clear	Bioptechs	0420041500C	coverglass bottom for optical compatibility
Disposable Pasteur Pipettes	VWR	14672-608	overall length 14.6 cm (53/4")
Dumont #5, #55, or #5SF Forceps	Fine Science Tools	11254-20	For style #5: straight tip, 0.05 x 0.01 mm tip, inox, 11 cm long
Flaming/Brown Micropipette Puller	Sutter	P-97	
Immersol W	Carl Zeiss Microscopy	4449690000000	immersion fluid for water-emission objectives, halogen-free, low fluorescence
Microinjection Mold	Adaptive Science Tools	TU-1	Six ramps, one 90 degree and one 45 degree beveled side.
Microloader Tips	Eppendorf	930001007	Microloader, tip for filling glass microcapillaries, $0.5 - 20\ \mu L$
mMessage mMachine SP6 Transcription Kit	Invitrogen	AM1340	contains SP6 Enzyme Mix, 10X Reaction Buffer, 2XNTP/CAP Solution, GTP Solution, pTRI-Xef, TURBO DNase, Ammonium Acetate Stop Solution, Lithium Chloride Precipitation Solution, and Gel Loading Buffer and are all stored at −20°C. Nuclease-free Water may be stored at any temperature.
Nikon SMZ645 Stereo Microscope	Nikon	SMZ645	used for injecting embryos (see Fig. 2B)
NotI-HF enzyme	NEB	R3189S	comes with Gel Loading Dye, Purple (6X)
NuSieve GTG Agarose	Lonza	50081	fine resolution, low melt agarose
Objective LD "C-Apochromat" 40x/1.1 W Korr M27	Carl Zeiss Microscopy	421867-9970-000	
Olympus SZX16 Stereo Microscope	Olympus	SZX2-ZB16	used for screening, embedding embryos (see Fig. 3A)
Phenol red solution	Sigma-Aldrich	P0290	0.5% in DPBS, sterile filtered, endotoxin tested, cell culture tested

Pico-liter Microinjector	Harvard Apparatus	PLI-100	Femtoliter to microliter injections; digital readouts for injection count, time, and pressure; contains 5 pressures including inject, balance, clear, fill, and hold
Pipette Pump Pipettor	SP Bel-Art	F37898	fits a disposable pasteur pipette, contains thumbwheel on side for aspirating or dispensing and plunger for quick emptying
Premium Thin Wall Borosilicate Glass Capillaries	Warner Instruments	G100T-4	1.0 x 0.78 mm
QIAquick PCR Purification Kit	Qiagen	28106	contains QIAquick Spin Columns, Buffers, Collection Tubes (2 ml)
RNase-free H2O	Invitrogen	AM9906	DNase-Free, Molecular Biology Grade, RNase-Free
RNeasy Mini Kit	Qiagen	74104	contains RNeasy Mini Spin Columns, Collection Tubes (1.5 ml and 2 ml), RNase-free Reagents and Buffers
Stage Attachment Z PIEZO WSB 500	Carl Zeiss Microscopy	432339-9000-000	
Stage Insert Z PIEZO WSB Universal	Carl Zeiss Microscopy	432339-9030-000	
Zeiss LSM 880 with Airyscan	Carl Zeiss Microscopy	N/A	inverted Axio Observer microscope
Zen Black 2.3 SP1 software	Carl Zeiss Microscopy	N/A	Zeiss Efficient Navigation (ZEN) controls all light microscope systems from Zeiss

Response to Reviewers JoVE62155 (Lusk, Casey, and Kwan)

We are very grateful to the reviewers for their positive comments and feedback on our manuscript. We also thank the editors for their careful attention to our manuscript. Please see below for our point-by-point to the comments and questions.

Editorial comments:
1. Please take this opportunity to thoroughly proofread the manuscript to ensure that there are no spelling or grammar issues. Please define all abbreviations at first use.
We have thoroughly proofread the manuscript.

2. Please revise the following lines to avoid overlap with previously published work: lines: 597-599
We have rephrased the movie legend.

3. JoVE cannot publish manuscripts containing commercial language. This includes trademark symbols (™), registered symbols (®), and company names before an instrument or reagent. Please remove all commercial language from your manuscript and use generic terms instead. All commercial products should be sufficiently referenced in the Table of Materials and Reagents.
For example: Zeiss LSM 80; QIAquick PCR Purification Kit; mMessage mMachine Transcription Kit; Airyscan; ZEN Black; Z-Pleizo; Nikon SMZ645, Olympus SZX16, FluoroRender, etc.
We have gone through and removed all of the commercial language from the manuscript. The exceptions to this are the following software names: ImageJ/FIJI, FluoRender, LongAxis, and LongTracker. These programs are not sold commercially; all of these were developed in academic settings and are freely available.

4. Please include an ethics statement before all of the numbered protocol steps indicating that the protocol follows the animal care guidelines of your institution.
The ethics statement has been moved to the beginning of the protocol section.

5. Please include a scale bar for all images taken with a microscope to provide context to the magnification used. Define the scale in the appropriate Figure Legend.
We have added scale bars where they were previously missing (Figures 2, 3), and have defined all scale bars in the Figure Legends.

6. As we are a methods journal, please add limitations of your technique as well to the Discussion section.
We have added Lines 754-758 to note that the protocol is limited in its scope and discuss limitations of our protocol and potential adaptations and optimizations throughout the Discussion and Introduction.

7. Please sort the Materials Table alphabetically by the name of the material.
We have now sorted the Materials Table alphabetically.

_____

Reviewers' comments:
Reviewer #1:
Manuscript Summary:

This is a clear and thorough protocol from the leader of the field of imaging zebrafish eye morphogenesis.

Major Concerns:
None

Minor Concerns:
1. It might be nice to mention what injection mold you use. Homemade? If purchased, provide source.
We apologize if this was not clear. The mold was purchased, and the details are in the Materials Table. We have added a note in Line 256 to point readers to the table.

Editorial:
1. Line 78. I would eliminate (or medaka). It just makes the next sentences confusing in regard to whether you are talking about zebrafish or medaka.
Thank you for this feedback; we have removed "(or medaka)" from the text.
2. Line 100. Should "in toto" be italicized?
We have now italicized "in toto" throughout the manuscript.
3. It is unclear why some sections are highlighted in yellow.
The highlighting is for the JoVE team.
4. Line 536. It looks like there is a line under the degree mark for 42oC.
Thank you for catching this; we have fixed this now.

Reviewer #2:
Manuscript Summary:
The manuscript by Lusk et al., provides a detailed description of how to perform live imaging of zebrafish early eye morphogenesis. The description is very thorough and includes all steps from generating synthetic mRNA for injection and labeling the embryo, through mounting and finally imaging.
The protocol is very well written and is sufficiently clear so it can be followed and repeated.

Minor Concerns:
1) Section 1.3. There additional reagents that can be used to purify RNA. It would be good to note this as some of the recommended reagents are very expensive and meant for large quantities (e.g. 50 preparations).
Thank you for your comment; this is obviously true. We have added a note at this step of the protocol (Lines 210-211) to point out the existence of alternative RNA purification methods.

2) Section 2.1.1 It would be useful to note that when storing injection agarose molds at 4 degrees it is good to have them covered with E3 medium so the agarose does not dry.
We agree that this is a very useful note, and we have now added this to the protocol in Section 2.1.1. (Lines 258-259).

3) Section 2.1.3 Concentration of phenol red is missing and also product information in the materials table.
Thank you for catching our oversight. We have added concentration information for phenol red in the protocol (0.1% final concentration, Line 275), and have added the product information to the Materials Table.

4) Section 3.1 line 276 concentration of gentamicin is missing and also product information in the materials table.

We have removed the gentamicin from the protocol, as this is actually not standard procedure in the lab.

5) How is optimal temperature maintained during the experiment?

This is a very good question, and we have added a note after 4.3.6, Lines 486-489. The additional text reads:

"NOTE: Although the confocal room is temperature controlled, the room temperature is 20-25 °C. With the equipment running and the lasers scanning, the temperature on the stage appears to be closer to 28.5 °C, since embryonic development proceeds at this expected rate, as assayed visually with morphological landmarks."

6) There are no labels in Figure 4 although labels are mentioned in the figure legend, lines 591-592.

Thank you very much for catching our oversight. We have now added labels to Figure 4 and information on the fluorescent labels in the Figure 4 legend.

7) In the last pages with the Table of Materials some of the text is cut and spreads over more than one page.

Thank you for alerting us to this; we have updated the table and fixed the formatting such that the text is no longer cut off.

Reviewer #3:
Manuscript Summary:
This is a very nice and easy-to-follow protocol for 4D in vivo imaging. The Kwan lab has pioneered many of these techniques and have generated a great protocol for those new to this type of imaging and/or even more skilled researchers who wish to expand on what they are currently doing. As such, it will be a nice publication and certainly benefit the field. I only have a couple of extremely minor comments; overall, this is a terrific manuscript/protocol.

Major Concerns:
NONE

Minor Concerns:
Lines 105/106 and 109 - you might provide REFs for the EGFP-CAAX and H2A.F constructs (or transgenic lines).

Thank you for catching our oversight. The EGFP-CAAX and H2A.F/Z-mCherry labeling is generated via RNA injection, and we have added a citation.

Line 131 - data "are" ideal

Thank you; we have fixed our grammatical error.

Section 1.4.4 – often on agarose gels, at least in my hands, mRNA runs as doublets – might be worth mentioning here

Thank you for this feedback; we have edited the language in Line 239 to reflect this.

Section 2.1 - people may not know what type of mold to use....any chance a CAD drawing is available?

We apologize if this was not clear in the manuscript. The mold was purchased, and the details are in the Materials Table. We have added a note in Line 256 to point readers to the table.

Section 2.1.2 -does the type of puller or filament (after ramp test) matter here? Might need to optimize settings when replaced.
We have included the settings and information for our particular needle puller. Many different methods can be used to pull needles, and the reviewer is correct that settings do indeed need to be optimized after replacing the filament. We have added a note to reflect this (Lines 267-268).

Reviewer #4:
Manuscript Summary:
In the present manuscript, Lusk and collaborators carefully describe the protocol they routinely use to inject mRNA and image zebrafish embryos. The Kwan lab has a long record providing some of the most impressive images of optic cup morphogenesis in the literature and, without a doubt, the techniques and tips detailed here will be useful in the field of retinal development. The details provided are comprehensive and easy to follow even for researchers not familiar with the system/model. The figures are helpful and beautifully put together. I unsuccessfully tried very hard to find flaws.

Minor Concerns:
1- The authors should define hpf in the abstract.
Thank you for catching our oversight; we have now defined hpf in the abstract.

2- Also, since the digestion time suggested for the DNA template is very long (overnight), they may wish to add a comment on the possibility of star activity.
Thank you for the suggestion. We have added a note after 1.1.1. to be aware of potential star activity (Lines 177-178).

3- line 295-296: clarify what is considered "super fine" forceps. Are Dumont #55 enough?
We have removed the word "super" from the manuscript, and in the Materials table, we add information for different forceps. In our experience, Dumont #5, #55 or #5SF are all suitable.

4- Line 353: "load pre-saved acquisition parameters" will not work for other labs, it's probably better to just define the parameters initially.
We thank the reviewer for this comment. We have removed this language and have simply included all of the parameters necessary for the confocal.